



Cyclosporine Biosynthesis in *Tolypocladium inflatum* Benefits Fungal Adaptation to the Environment

Xiuqing Yang,^{a,b} Peng Feng,^a Ying Yin,^a Kathryn Bushley,^c Joseph W. Spatafora,^d  Chengshu Wang^{a,e}

^aKey Laboratory of Insect Developmental and Evolutionary Biology, CAS Center for Excellence in Molecular Plant Sciences, Shanghai Institute of Plant Physiology and Ecology, Chinese Academy of Sciences, Shanghai, China

^bUniversity of Chinese Academy of Sciences, Beijing, China

^cDepartment of Plant Biology, University of Minnesota, St. Paul, Minnesota, USA

^dDepartment of Botany and Plant Pathology, Oregon State University, Corvallis, Oregon, USA

^eSchool of Life Science and Technology, ShanghaiTech University, Shanghai, China

ABSTRACT The cycloundecapeptide cyclosporin A (CsA) was first isolated from the insect-pathogenic fungus *Tolypocladium inflatum* for its antifungal activity and later developed as an immunosuppressant drug. However, the full biosynthetic mechanism of CsA remains unknown and has puzzled researchers for decades. In this study, the biosynthetic gene cluster is suggested to include 12 genes encoding enzymes, including the nonribosomal peptide synthetase (NRPS) (SimA) responsible for assembling the 11 amino acid substrates of cyclosporine and a polyketide synthase (PKS) (SimG) to mediate the production of the unusual amino acid (4*R*)-4-[(*E*)-2-butenyl]-4-methyl-L-threonine (Bmt). Individual deletion of 10 genes, isolation of intermediates, and substrate feeding experiments show that Bmt is biosynthesized by three enzymes, including SimG, SimI, and SimJ. The substrate D-alanine is catalyzed from L-alanine by alanine racemase SimB. Gene cluster transcription is regulated by a putative basic leucine zipper (bZIP)-type protein encoded by the cluster gene *SimL*. We also found that the cluster cyclophilin (*SimC*) and transporter (*SimD*) genes contribute to the tolerance of CsA in the CsA-producing fungus. We also found that cyclosporine production could enable the fungus to outcompete other fungi during cocultivation tests. Deletion of the CsA biosynthetic genes also impaired fungal virulence against insect hosts. Taking all the data together, in addition to proposing a biosynthetic pathway of cyclosporines, the results of this study suggest that CsA produced by this fungus might play important ecological roles in fungal environment interactions.

IMPORTANCE The cyclopeptide cyclosporin A was first isolated from the filamentous fungus *Tolypocladium inflatum* showing antifungal activity and was later developed as an immunosuppressant drug. We report the biosynthetic mechanism of cyclosporines that are mediated by a cluster of genes encoding NRPS and PKS controlled by a bZIP-type transcriptional regulator. The two unusual amino acids Bmt and D-Ala are produced by the PKS pathway and alanine racemase, respectively. The cyclophilin and transporter genes jointly contribute to fungal self-protection against cyclosporines. Cyclosporine confers on *T. inflatum* the abilities to outcompete other fungi in competitive interactions and to facilitate fungal infection of insect hosts, which therefore benefits fungal adaptations to different environments.

KEYWORDS cyclosporine, *Tolypocladium inflatum*, antifungal activity, biosynthetic pathway, virulence

Received 1 June 2018 Accepted 22 August 2018 Published 2 October 2018

Citation Yang X, Feng P, Yin Y, Bushley K, Spatafora JW, Wang C. 2018. Cyclosporine biosynthesis in *Tolypocladium inflatum* benefits fungal adaptation to the environment. *mBio* 9:e01211-18. <https://doi.org/10.1128/mBio.01211-18>.

Editor B. Gillian Turgeon, Cornell University

Copyright © 2018 Yang et al. This is an open-access article distributed under the terms of the [Creative Commons Attribution 4.0 International license](https://creativecommons.org/licenses/by/4.0/).

Address correspondence to Chengshu Wang, cswang@sibs.ac.cn.

Cyclosporine (CSN) was first isolated and structurally identified as a cyclic undecapeptide metabolite from the insect-pathogenic and soil-dwelling fungus *Tolypocladium inflatum* in the early 1970s (1, 2). Cyclosporin A (CsA) was developed and approved as an immunosuppressant drug used in organ transplantation in 1983, and more than 30 analogs of CsA have been identified with different biological activities, including immunosuppressive, antifungal, antiviral, and antiparasitic properties (3).

Due to the high value of CsA, scientists have been attempting to dissect its biosynthetic mechanism for decades. In the early 1990s, the nonribosomal peptide synthetase (NRPS) gene (termed *SimA*) was cloned, and its role in CSN biosynthesis was functionally confirmed (4, 5). However, the biosynthetic pathway of CSN is still unclear. CsA is composed of 11 amino acids, including two nonproteinogenic substrates D-alanine (D-Ala) and (4R)-4-[(E)-2-butenyl]-4-methyl-L-threonine (Bmt). An alanine racemase (AlaR) with a high activity in conversion of L-Ala to D-Ala was previously purified from *T. inflatum* and shown to have a role in CSN biosynthesis (6, 7). Bmt has been characterized biochemically and proposed to be produced by a polyketide synthase (PKS) (8–10). On the basis of different methods of prediction and gene expression analysis, 10, 14, or 22 genes have been proposed for the CsA biosynthetic gene cluster (1). The functions of these genes have not been investigated until now.

CsA was first characterized as an antifungal compound (3). Thus, CsA production can be toxic to the producing fungus *T. inflatum*. The target of CsA was first determined as cyclophilin A (CypA) which exhibits a peptidyl-prolyl isomerase activity (11). Multiple cyclophilin genes are present in different organisms and have been found to play diverse biological roles, including stress tolerance, signal transduction, gene regulation, and pathogenesis (12). For example, 11 cyclophilin genes were characterized to alternatively mediate fungal conidiation, heat tolerance, virulence, and sensitivity/resistance to CsA in the insect pathogen *Beauveria bassiana*, a close relative of *T. inflatum* (13). It was hypothesized that the CsA binding feature of cyclophilin could potentiate the tolerance of *T. inflatum* cells against the CSN products (3, 14). It was found that a cyclophilin gene within the CsA biosynthetic gene cluster was highly expressed by the fungus in both a CSN induction medium and a medium containing insect hemolymph (1). However, the protective effect of this gene on CsA cytotoxicity has not been verified. It is unknown whether there is any other gene (e.g., the membrane transporter) that also contributes to self-tolerance/detoxification of CsA. The CSN producer *T. inflatum* is a pathogen of beetles (1). It has been reported that CsA could inhibit insect immune responses by targeting lipophorins, the regulators of both humoral and cellular immune responses in insects (15, 16). The contribution of CSNs to fungal virulence remains to be determined.

In this study, using the predicted biosynthetic gene cluster from the genome sequence, we performed multiple gene deletions and intermediate isolation and substrate feeding experiments to dissect the CsA biosynthetic mechanism in *T. inflatum*. We also explored the possible adaptive functions of CSNs to the CSN-producing fungus by conducting fungal competition tests and insect bioassays. We find that CSNs allow the producing fungus to outcompete other fungi and facilitates fungal infection of insect hosts.

RESULTS

Functional verification of the clustered genes. On the basis of our previous predictions (1), 15 genes were investigated, and 12 of the genes were named *SimA* to *SimL* for the putative biosynthetic gene cluster of CSNs (Fig. 1A). This gene cluster is predicted to encode the enzymes NRPS (*SimA*) and PKS (*SimG*) as well as the alanine racemase (*SimB*), cyclophilin (*SimC*), ABC transporter (*SimD*), cytochrome P450 (*SimI*), aminotransferase (*SimJ*), and transcription factor (TF) (*SimL*). Additional analysis of the previously annotated gene *TINF00195* suggested that it is unlikely to encode a functional dehydrogenase, as its open reading frame is only 198 nucleotides. *TINF00195* was not further examined. The hypothetical protein genes *SimF*, *SimH*, and *SimK* were also excluded in further analysis due to their unclear functional contributions to CSN

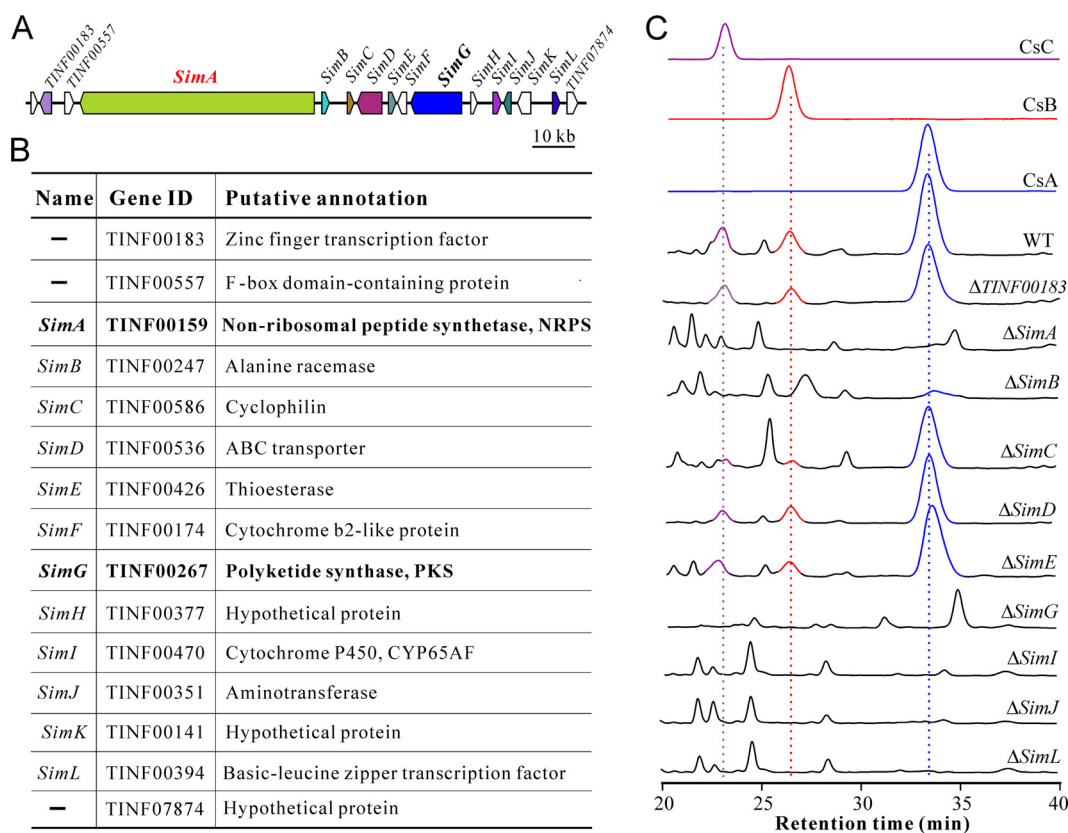


FIG 1 Prediction and functional verification of the CSN biosynthetic gene cluster. (A) Schematic map of the biosynthetic gene cluster. The genes are named following the previously designated *SimA* gene for the core NRPS gene. (B) Annotation of the gene contents within the gene cluster. ID, identifier. (C) Loss-of-function verification of the contributions of different genes to CSN biosynthesis. HPLC analysis of CSN production by the WT and different null mutants of *T. inflatum*. The standards CsA, CsB, and CsC were included in parallel analysis.

biosynthesis. *SimE* (previously predicted to be an esterase-like protein) contains a putative thioesterase (TE) domain (Pfam00975; 1.13×10^{-7}) (Fig. 1B). To determine the boundary of the gene cluster and the contributions of these genes to CSN biosynthesis, 10 genes were individually deleted by homologous recombination via *Agrobacterium*-mediated transformation of the wild-type (WT) strain of *T. inflatum* (see Fig. S1 in the supplemental material), including a putative zinc finger TF *TINF00183* gene upstream of *SimA*. After growth in the CSN induction medium containing fructose (fructose CSN induction medium) (17), high-performance liquid chromatography (HPLC) analysis demonstrated that the WT strain could produce CsA, cyclosporin B (CsB), and cyclosporin C (CsC) during chromatographic profiling with these standards. Extracts of mutants lacking either *SimA*, *SimG*, *SimI*, *SimJ*, or *SimL* resulted in the failure to detect CsA to CsC (Fig. 1C). Disruption of the putative racemase gene *SimB* impaired but did not completely abolish fungal ability to produce CsA. No obvious differences were observed between WT and null mutants of *SimC*, *SimD*, *SimE*, or *TINF00183* in CSN production.

Conversion of L-Ala to substrate D-Ala. Previously, it was reported that the putative racemase encoded by *SimB* (referred to originally as *AlaR*; GenBank accession no. A40406) was able to convert L-Ala to D-Ala (7). We found that deletion of *SimB* significantly reduced but did not completely abolish CSN production in *T. inflatum* (Fig. 1C). It was previously noted that synthesis of D-Ala could also be mediated by a threonine aldolase (7). Analysis of the *T. inflatum* genome sequence identified a putative threonine aldolase (TINF06009; sharing 43% identity with *SimB* at the amino acid level), located outside the putative CsA biosynthetic gene cluster. To verify the potential contribution of this gene, deletion of *TINF06009* was conducted in the $\Delta SimB$

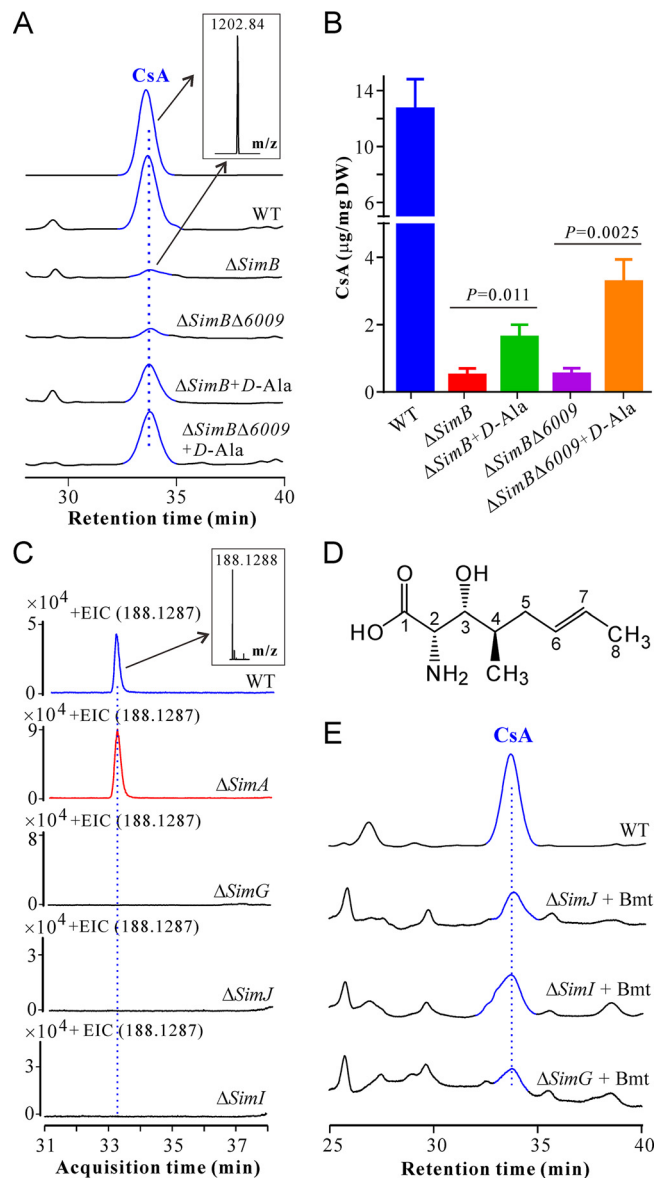


FIG 2 Verification of the genes involved in D-Ala conversion and Bmt biosynthesis. (A) HPLC analysis of CsA production by WT and different mutants with or without the addition of D-Ala. The inset shows the mass spectra detected for the CsA and $\Delta SimB$ samples. m/z , $[M+H]^+$; $\Delta SimB\Delta 6009$, $\Delta SimB \Delta TINF06009$ double mutant. (B) Quantification analysis of CsA production by WT and different mutants. The strains were grown in fructose CSN induction medium with or without the supplementation of D-Ala (at a final concentration of 20 mM) for 10 days. The mycelia were then harvested for CSN extraction. Values are means plus standard errors (SE) (error bars). DW, mycelium dry weight. (C) LC-MS analysis of the extracted ion chromatography (EIC) showing the production or nonproduction of Bmt by WT and mutant strains. m/z , $[M+H]^+$. (D) Chemical structure of Bmt. (E) Supplementation of Bmt (at a final concentration of 85 μM) in the growth medium enabled the null mutants to produce CsA (peaks shown in blue).

background for a double deletion of these two genes. HPLC analysis revealed that trace amounts of CsA could still be produced by the double mutant ($\Delta SimB \Delta TINF06009$ [$\Delta SimB\Delta 6009$]) (Fig. 2A). We also performed feeding assays and found that supplementation of D-Ala could significantly increase the cellular accumulation of CsA by both $\Delta SimB$ ($P = 0.011$) and $\Delta SimB\Delta 6009$ ($P = 0.0025$) mutants compared with the corresponding null mutants growing in the medium without D-Ala. Unexpectedly, feeding with D-Ala could not fully enable the mutants to produce the same amount of CsA as the WT did, for unknown reasons (Fig. 2B).

Bmt biosynthesis. We found that deletion of the PKS gene *SimG* abolished the fungal ability to produce CSNs (Fig. 1C). It is hypothesized that a PKS could be responsible for the biosynthesis of the Bmt with a deduced structure 3*R*-hydroxyl-4*R*-methyl-6*E*-octenoic acid (termed compound b1) (9). We performed liquid chromatography (LC)-mass spectrometry (MS) analysis of both the WT and mutant samples in order to detect Bmt or other similar carboxylic acid type intermediates. It was found that, relative to the WT, $\Delta SimG$, $\Delta SimJ$, and $\Delta SimI$ mutants lost the abilities to produce a compound with a $[M+H]^+$ molecular ion of 188.1288, which was more highly accumulated in the $\Delta SimA$ mutant than in the WT (Fig. 2C). This chemical was then purified based on its mass through two rounds of preparative LC-MS analysis, and the obtained compound was subjected to one-dimensional (1D) and two-dimensional (2D) nuclear magnetic resonance (NMR) analysis (Fig. S2 and S3). The data obtained revealed that this compound is Bmt (Fig. 2D; see also Table S1 in the supplemental material). Unfortunately, efforts to isolate the predicted Bmt precursors b1 to b3 were not successful, given that the isoabsorbance plot profiles were different for the mutants in HPLC analysis equipped with a diode array detector (DAD) (Fig. S4). We also conducted substrate feeding assays with the purified Bmt and found that the supplementation of Bmt could restore the ability of all three mutants, $\Delta SimG$, $\Delta SimJ$, and $\Delta SimI$ mutants, to produce CsA (Fig. 2E). Thus, taken together, Bmt is likely the product of the following biochemical pathway: *SimG* to *SimI* to *SimJ*, an intermediate in the production of CsA.

Pathway-specific regulation control. Fungal secondary metabolism is controlled by both global regulator(s) and/or pathway-specific TFs (18, 19). There are two TFs (i.e., *TINF00183* and *SimL*) in close proximity to the CsA gene cluster. Our previous transcriptome sequencing (RNA-seq) analysis indicated that the expression of *TINF00183* was not upregulated in an inductive medium (1). To explore a possible role in CsA biosynthesis, deletion mutants of these putative TFs was generated. Analysis of mutant extracts revealed that the basic leucine zipper (bZIP)-type TF *SimL*, but not the zinc finger TF *TINF00183*, controlled CSN production (Fig. 1C). To further confirm the function of *SimL*, we performed gene overexpression. Thus, *SimL* was put under the control of the constitutive glyceraldehyde-3-phosphate dehydrogenase (*GpdA*) gene (*TINF02918*) promoter, and the cassette was used to transform the WT strain of *T. inflatum*. Three independent transformants were selected for trial evaluations of CsA production, and the one with the highest yield was used for further analysis. After the fungi were grown in the fructose CSN induction medium for 10 days, RNAs were extracted for semiquantitative reverse transcription-PCR (RT-PCR) analysis. Consistent with the results of our previous RNA-seq analysis (1), the results indicated that the clustered genes were co-upregulated, with the cyclophilin gene *SimC* being the most highly transcribed by the fungus (Fig. 3A). Except for *SimC*, *SimK*, *TINF00183*, and *TINF07874*, deletion of *SimL* deactivated the expression of other genes. In contrast, overexpression of *SimL* highly induced the transcription of the cluster genes compared with the WT strain (Fig. 3A).

The characteristic binding motif of fungal bZIP-type TFs is TGACG (20). *In silico* analysis identified the presence of this conserved motif in the promoter regions of the clustered genes (Fig. 3B). Quantification analysis of CsA production also revealed that *SimL* overexpression significantly ($P = 0.0091$) increases the yield of CsA production (26.15%) (Fig. 3C). Taken together, the data indicate that *SimL* is responsible for the pathway-specific control of CSN biosynthesis in *T. inflatum*.

Deduction of the biosynthetic pathway. Having determined functions of several genes in the cluster, we next tried to deduce the CsA biosynthetic pathway. As indicated above, *SimG*, *SimI*, and *SimJ* are all required for the production of Bmt (Fig. 1C and Fig. 2E). It is likely that the PKS *SimG* mediates the biosynthesis of compound b1 from acetyl coenzyme A (acetyl-CoA), malonyl-CoA, and *S*-adenosylmethionine, and compound b1 will then be repeatedly oxidized by *SimI* to 3*R*-hydroxy-4*R*-methyl-2-keto-6*E*-octenoic acid (compound b3). The latter is likely converted to Bmt through the action of the aminotransferase *SimJ* (Fig. 4A).

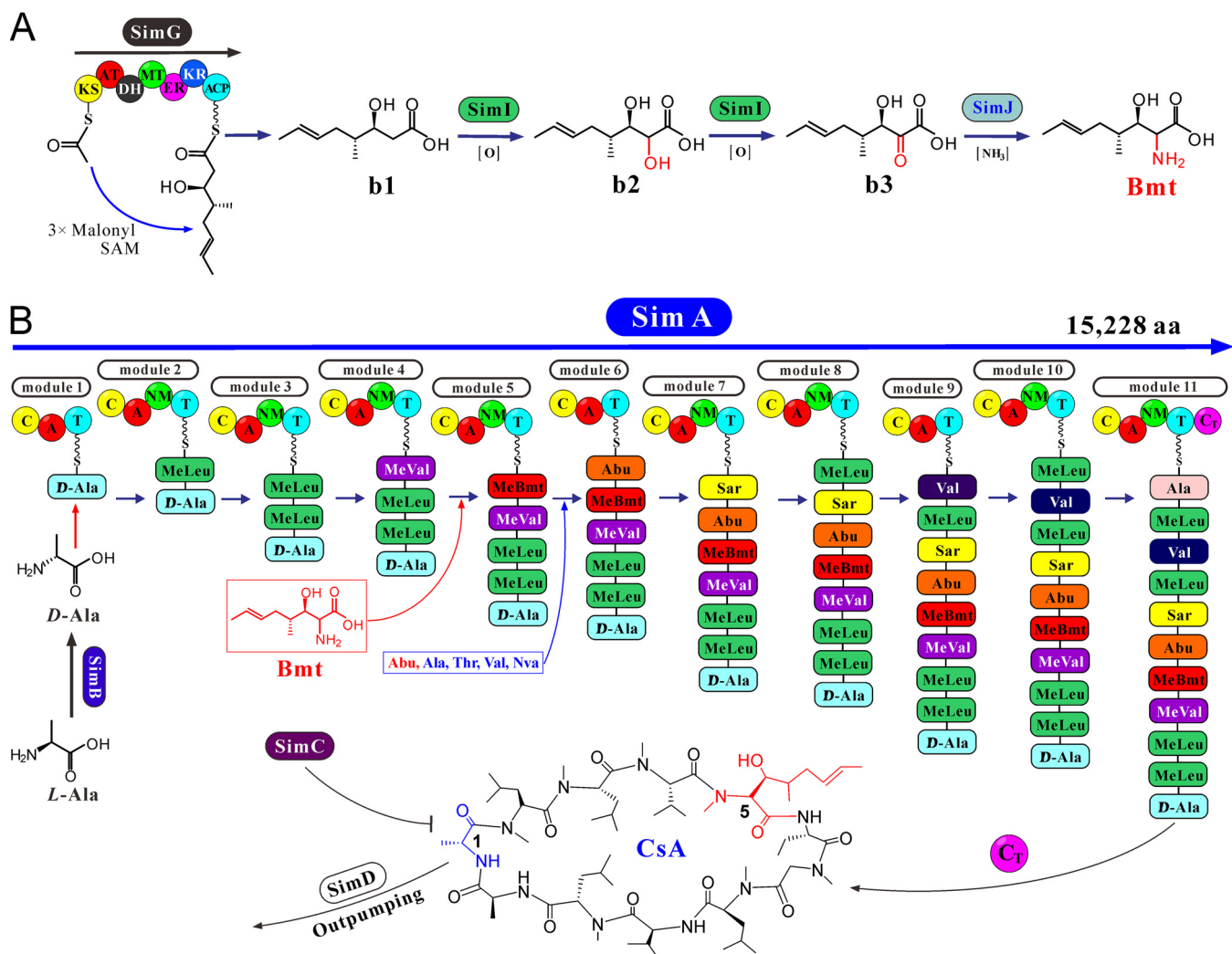


FIG 4 Proposed pathway for CsA biosynthesis. (A) Bmt biosynthesis by the PKS pathway. The PKS SimG domains include the following: β -ketoacyl synthase (KS), acyltransferase (AT), dehydrogenase (DH), methyltransferase (MT), enoylreductase (ER), ketoreductase (KR), acyl carrier protein (ACP), *S*-adenosylmethionine (SAM). The chemical structure of compounds b1 to b3 and Bmt are shown. (B) Schematic structure of NRPS SimA and the machinery of CsA biosynthesis. There are 11 modules of SimA, and each module contains the condensation (C), adenylation (A), thiolation (T), and/or *N*-methylation (NM) domains. The terminal C domain (C_T) is implicated in cyclization of the peptidyl chains to form CsA and its analogs. The cyclophilin SimC and exporter SimD may jointly contribute to cell tolerance of CSNs. Abu, aminobutyric acid; Sar, sarcosine; Nva, norvaline; MeLeu, methylleucine; aa, amino acids.

Cyclophilin and transporter genes mediate fungal self-protection against CSNs.

CypA is the immediate receptor of CsA in humans (3). Within the biosynthetic gene cluster, *SimC* encodes a cyclophilin. Deletion of *SimC* had no obvious effect on CSN biosynthesis in *T. inflatum* (Fig. 1C). *SimC* is similar to human cyclophilin A (NCBI:protein accession no. P62937; 62% amino acid identity), and the gene was highly transcribed by the fungus grown in a CSN induction medium (Fig. 3A), evidence suggesting that *SimC* plays a role in cell self-protection from CSNs (3). To test this, we performed growth rate assays on a potato dextrose agar (PDA) with or without the addition of CsA for 2 weeks (Fig. S6A). Relative to the WT, the growth rate of the $\Delta SimC$ mutant was significantly reduced, whereas the growth rate of the $\Delta SimA$ mutant was significantly increased ($P < 0.001$) (Fig. S6B). Therefore, we suggest that as CSNs are toxic to other fungi and also to the producing fungus *T. inflatum*, *SimC* may function to bind CSN to reduce toxicity and increase cell tolerance of the accumulated cyclopeptides. The results also indicated that the addition of CsA significantly ($P < 0.001$) inhibited the growth of the examined WT, $\Delta SimC$, $\Delta SimA$, and $\Delta SimD$ strains compared with the growth on PDA. Besides *SimC*, nine additional cyclophilin genes, including a

highly similar paralog TINF04375 (63% identity), were identified in the genome of *T. inflatum* (1). These proteins are separated in different lineages (Fig. S7). It is not clear whether the closely related cyclophilins may play an additional or redundant role in fungal self-protection.

We found that deletion of the ABC transporter gene *SimD* resulted in a higher ($P = 0.0147$) level of cellular CsA accumulation but a lower ($P = 0.0287$) level of CsA in the culture filtrates compared with the WT (Fig. S6C and D). The growth rates of WT and $\Delta SimD$ mutant had no obvious difference on PDA, but the latter was significantly ($P = 0.0023$) inhibited on CsA-amended PDA compared with the WT (Fig. S6B). The results indicated that *SimD* functions as an exporter and may jointly contribute to the resistance of CSNs in *T. inflatum*.

CsA production benefits fungal competition against other fungi. Given that CsA has antifungal activity (3), we performed fungal competition tests by cocultivation of the WT and different mutants of *T. inflatum* with the saprophytic fungus *Aspergillus flavus* (Fig. 5A). After measuring the colony edge distance 1 week postinoculation (Fig. 5B), comparative analysis revealed that the distance between the WT *T. inflatum* and *Aspergillus* was significantly larger ($P < 0.001$) than those between CsA-nonproducing mutants ($\Delta SimA$, $\Delta SimG$, and $\Delta SimL$) and the mold fungus (Fig. 5C). The pairwise comparison between WT and CsA-producing mutants (*SimC*, *SimD*, and WT::*SimL*) found no difference 1 week postinoculation (Fig. 5C and D). However, the overexpression mutant of *SimL* inhibited *Aspergillus* growth more significantly ($P < 0.001$) than did the WT after growth for 14 days (Fig. 5D). A competitive advantage could be more clearly observed such as between WT and $\Delta SimA$ after the fungi were grown for up to 3 weeks (Fig. 5E). Further cocultivation tests against other insect-pathogenic fungi, i.e., the close relatives/competitors of *Tolypocladium*, also revealed that the WT demonstrated stronger antifungal activity than the $\Delta SimA$ mutant did (Fig. S8). Thus, the production of CSNs can benefit *T. inflatum* by conferring its ability to outcompete other fungi in the environment.

CsA production is required for fungal full virulence. To determine the contribution of CsA production to fungal virulence, we conducted insect bioassays by injecting a spore suspension into the last instar larvae of wax moth (*Galleria mellonella*) (Fig. 6A). The estimation of median lethal time (LT_{50}) indicated that the LT_{50} values of $\Delta SimA$, $\Delta SimG$, and $\Delta SimL$ mutants were significantly higher than that of the WT, i.e., the null mutants became less virulent. However, the difference between WT and WT::*SimL* was insignificant (Fig. 6B). Consistent with the suppressive effect of CsA on insect immunities (16), the data indicated therefore that CsA production plays a role in fungal infection of insect hosts.

DISCUSSION

After the development of CsA as a commercial immunosuppressant drug, decades-long efforts have attempted but failed to uncover the full mechanism of CsA biosynthesis (5). In this study, we propose the biosynthetic mechanism, regulation control, self-protection strategy, and chemical ecology of CSN production in *T. inflatum*. Ten genes were selected for loss-of-function studies by excluding a misannotated artifact and four hypothetical genes. We verified that the bZIP-type transcription factor (TF) *SimL*, but not the zinc finger TF TINF00183, mediates the pathway-specific regulation of cyclosporine (CSN) production in *T. inflatum*. Thus, overexpression of *SimL* could substantially increase the biosynthetic titer of CSNs in the fungus. Taken together with the RT-PCR analysis of gene expression levels in $\Delta SimL$ and WT::*SimL* strains (Fig. 3A), the genes located upstream of *SimA* and downstream of *SimL* are unlikely to belong to the CsA biosynthetic cluster.

We found that deletion of the thioesterase (TE)-like gene *SimE* had no obvious effect on CSN production in *T. inflatum* (Fig. 1C). In bacteria, however, deletion of the free TE gene within a cluster significantly reduced metabolite production (22). It has been found that additional TE genes in either the PKS or NRPS gene cluster could not compensate for the catalysis of compound termination/cyclization mediated by the

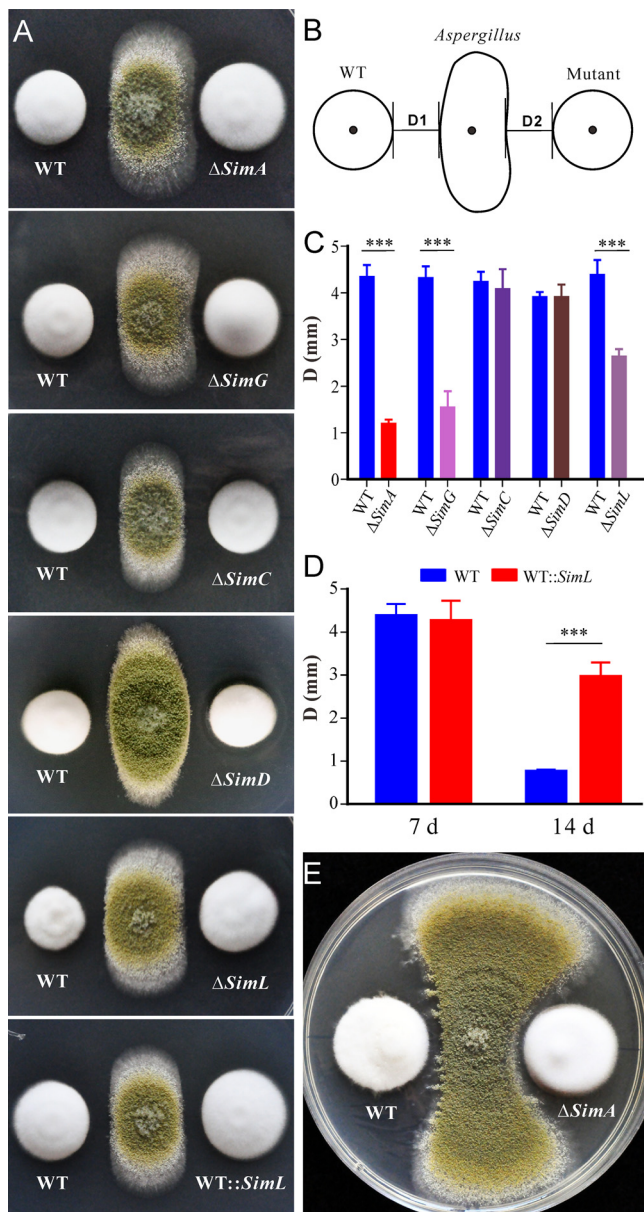


FIG 5 Antifungal effect of CsA production. (A) Fungal cocultivation tests. The WT and mutants of *T. inflatum* were inoculated on PDA plates in parallel for 3 days, and the strain of *A. flavus* was then inoculated between the two *T. inflatum* colonies for 4 days. (B) Schematic diagram showing how the colony edge distances between the WT *T. inflatum* and *Aspergillus* (D1) or between the *T. inflatum* mutant and *Aspergillus* (D2) were measured. (C) Comparison of the colony edge distances between strains. Values are means plus SE. Values that are significantly different ($P < 0.001$ by two-tailed *t* test) are indicated by a bar and three asterisks. (D) Comparison of the colony edge distances between WT and WT::SimL strains after different incubation times (7 or 14 days [d]). Values are means plus SE. ***, $P < 0.001$. (E) Representative phenotypes of a fungal pair after inoculation and 3 weeks of growth of *T. inflatum*.

integral TE domain found at the end of core PKS or NRPS enzymes. Instead, the free TE gene may fulfill an editing function during metabolite biosynthesis (22). We found that the terminal C domain of SimA could be grouped together with those C_T domains being functionally verified to catalyze the cyclization of macrocycles, e.g., the C_T domain of the NRPS TqaA from *Penicillium aethiopicum* (21, 23). It is suggested therefore that the terminal C domain of SimA might contribute to the release and cyclization of CSNs. The exact function of SimE remains to be determined. In addition, since the expression of the hypothetical genes SimF and SimH is similarly regulated by

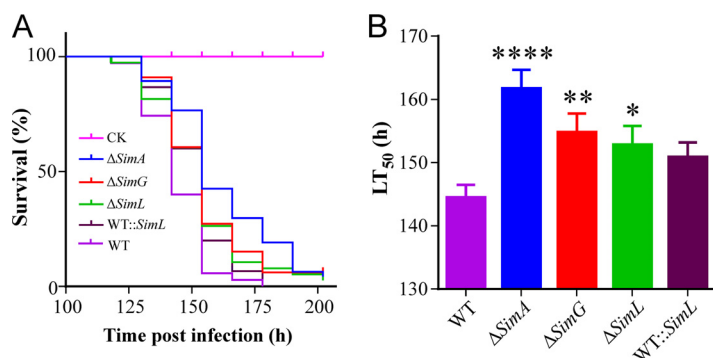


FIG 6 Insect bioassays. (A) Survival of insects after injection with the spores of the WT and different mutants. Control insects (CK) were injected with 0.05% Tween 20. (B) Comparison of the LT_{50} values for the WT and different mutants. Values are means plus SE. Values that are significantly different from the value for the WT by log rank tests are indicated by asterisks as follows: ****, $P < 0.0001$; **, $P = 0.0087$; *, $P = 0.0182$.

SimL, future studies are still required to determine the functions of these predicted protein genes. Considering that the cluster genes are differentially regulated by SimL in the WT strain and that the expression of *SimC* and *SimK* could still be detected in the $\Delta SimL$ mutant (Fig. 3A), the possibility that additional TF(s) may be involved in jointly controlling the biosynthesis of CSNs cannot be ruled out.

Nine of eleven amino acids in CsA are nonproteinogenic, including the D-Ala, Bmt, L-aminobutyric acid (Abu), sarcosine (Sar) (*N*-methylglycine), and *N*-methylated leucine and methylvaline. *In situ* *N*-methylation can be mediated by the NM domains encoded in the corresponding modules of SimA (Fig. 4B). Our genome survey indicated that a single copy of the AlaR gene (*SimB*) is present in the genome of *T. inflatum*. Thus, consistent with the biochemical study using the purified AlaR enzyme (6), gene deletion and substrate feeding assays confirmed that SimB contributes to D-Ala conversion (Fig. 2A). Intriguingly, we found that trace amounts of CsA could still be produced by the $\Delta SimB$ mutant and the double mutant with both the *SimB* and threonine aldolase (*TA*) genes deleted. In contrast, deletion of *ToxG* (42% identity to SimB at the amino acid level) in the plant pathogen *Cochliobolus carbonum* completely abolished the production of the D-Ala-containing form of HC toxin (24). No alternative substitute is found in place of D-Ala in the structures of CSNs (3). Thus, an additional source of D-Ala remains to be determined in *T. inflatum*. It is also unclear why feeding D-Ala failed to restore the abilities of the $\Delta SimB$ and $\Delta SimB\Delta 06009$ mutants to produce the WT level of CsA (Fig. 2B). Structurally, CsA (Abu) differs from CsB (Ala) and CsC (Thr) only at position 6 (Fig. 4B). Abu can be converted from Thr through the function of threonine deaminase (25). A yeast ILV1-like threonine deaminase is present in *T. inflatum* (TINF04164, 50% amino acid identity). This gene is not present in the *SimA* cluster, implying that Abu could be synthesized outside the cluster for CsA biosynthesis. Regarding the PKS pathway for Bmt biosynthesis, different DAD-chromatographic profiles (isoabsorbance plots) could at least be observed between the $\Delta SimG$ mutant and the $\Delta SimI/\Delta SimJ$ mutant and between the $\Delta SimI$ and $\Delta SimJ$ mutants (see Fig. S4 in the supplemental material). Future efforts are still required to determine the oxidation function of SimI and verify the structure of the proposed intermediates.

Accumulated evidence has indicated that the small molecules produced by different fungi as well as bacteria play important roles in the environmental adaptation and competitive advantage of the organisms producing the molecules. However, except for the perceived biological properties, the ecological importance of many metabolites is largely unknown (26). A few secondary metabolites produced by insect-pathogenic fungi have been established to contribute to fungal virulence against insect hosts such as the destruxins produced by *Metarhizium* species (27) and the beauvericin and oosporein biosynthesized by *Beauveria bassiana* (28, 29). The oosporein produced by

Beauveria could also help the fungus to outcompete bacterial growth during fungal colonization of insect hosts (30, 31). Consistent with the immune inhibition and insecticidal effect of CsA on insects (16, 32), our insect bioassays revealed that abolishment of CSN production impaired fungal virulence against insect hosts. In this study, we also established that the production of CSNs can enable the CSN-producing fungus *T. inflatum* to outcompete other fungi in the environment. However, the exact mechanisms of CSN ecological functions required further investigations.

In conclusion, we report the biosynthesis of CSNs that is regulated by a bZIP-type TF SimL in *T. inflatum*. It is indicated in this study that the cyclophilin and transporter genes encoded in the *SimA* cluster contribute to the self-protection/tolerance of CSNs in the CSN-producing fungus. On the other hand, CSN production benefits the fungus by allowing it to outcompete other fungi and facilitate fungal infection of insect hosts. In addition to suggesting the CSN biosynthetic pathway, the results of this study advance our understanding of the ecological role of this important drug molecule to fungal adaptations in the environment.

MATERIALS AND METHODS

Fungal strains and reagents. The wild-type (WT) strain NRRL 8044 (ATCC 34921) of *Tolypocladium inflatum* (1) was used to generate the gene deletion mutants. Both the WT and mutants were maintained either on potato dextrose agar (PDA) (BD Difco) or in a Sabouraud dextrose broth (SDB) (BD Difco). For induction of CsA production, the WT or mutants was induced in the cyclosporine (CSN) induction medium containing fructose (fructose CSN induction medium) [fructose, 30 g/liter; (NH₄)₂HPO₄, 6 g/liter; yeast extract, 5 g/liter; CaCl₂·2H₂O, 1.32 g/liter; MgSO₄·7H₂O, 2.05 g/liter; FeSO₄·7H₂O, 27.4 mg/liter; ZnSO₄·7H₂O, 17.8 mg/liter; CoCl₂·6H₂O, 27.5 mg/liter; CuSO₄·5H₂O, 3.1 mg/liter] adjusted from a previous study (17). The strains of *Aspergillus flavus* (NRRL 3357), *Metarhizium robertsii* (ARSEF 23) (33), *Cordyceps cicadae* (CCAD02) (34), *Cordyceps militaris* (Cm01) (35), and *Beauveria brongniartii* (RCEF 3172) (36) were used for antifungal assays between WT and null mutants of *T. inflatum*. The standards of cyclosporin A (CsA) and D-Ala were ordered from Sigma-Aldrich (USA), and CsB and CsC were purchased from Santa Cruz Biotechnology (USA).

Gene deletion, overexpression, and fungal transformation. To determine the functions of the clustered genes, gene deletions were individually performed by using *Agrobacterium*-mediated transformation of *T. inflatum* (37). To generate the deletion vectors, the 5'- and 3'-flanking regions of the target gene were amplified by PCR using different primer pairs (see Table S2 in the supplemental material). For example, primers SimA-U1/SimA-U2 (U stands for upper strand) were used to amplify the *SimA* upstream region, and primers SimA-L1/SimA-L2 (L stands for lower strand) were used to amplify the *SimA* downstream region. The PCR fragments obtained were treated with the restriction enzymes, purified, and then cloned into the same enzyme-treated binary vector pDHT-SK-Bar (28) for *Agrobacterium*-mediated transformation of the WT strain. For double deletion of *SimB* and the putative threonine aldolase (TA) gene *TINF06009*, the flanking regions of *TINF06009* were amplified by fusion PCRs with the ClonExpress II one step cloning kit (Vazyme, China), and the products were cloned into the binary vector pDHT-SK-Ben (28) for transformation of the Δ *SimB* mutant. The drug resistance colonies were verified by PCR, and reverse transcription-PCR (RT-PCR) was performed to verify gene deletions after single spore isolation. For overexpression of the transcription factor SimL in the WT strain, the full-length open reading frame (ORF) of this gene was amplified using the genomic DNA of *T. inflatum* as a template by fusion PCRs with different primers using the ClonExpress kit. The gene was made under the control of the constitutive GpdA gene (*TINF02918*) promoter, and the cassette was cloned into the pDHT-SK-Bar plasmid for transformation of the WT strain of *T. inflatum*.

Gene expression profiling and scanning of the putative binding site of SimL. To determine gene expression control by SimL, the WT, Δ *SimL*, and WT::*SimL* strains were grown in the fructose CSN induction medium for 10 days. The mycelia were harvested, washed twice with sterile water, and homogenized in liquid nitrogen for RNA extraction with the TransZol UP Plus RNA kit (Transgen Biotech, China) by following the manufacturer's protocol. The RNA (20 μ g each) was then converted to cDNA using the ReverTra Ace quantitative PCR (qPCR) real-time (RT) master mix (Toyobo Life Science, Japan). Semiquantitative RT-PCR analysis was performed using the primer pairs for different genes (Table S2). A β -tubulin gene (*TINF09088*) of *T. inflatum* was amplified as a reference. The conserved binding motif of the fungal basic leucine zipper (bZIP)-type transcription factor (TF) was identified to be 5'-TGACG-3' (20). To examine the presence or absence of this motif, the promoter region (1 to 1.5 kb upstream of the start codon) of the cluster gene was scanned. Each identified motif was extracted together with its flanking sequences (five nucleotides) to generate the sequence logo using WebLogo 3 (38).

Induction of CSN production and chromatography analysis. The conidial spores of the WT and different mutants of *T. inflatum* were harvested from *T. inflatum* cultures grown on PDA plates for 4 weeks and suspended in 0.05% Tween 20 to a final concentration of 1×10^8 spores/ml. The spores were inoculated (50 μ l each) into the fructose CSN induction medium (50 ml in each flask; pH 5 to 6) and incubated in a rotatory shaker at 25°C and 200 rpm for 10 days. For D-Ala feeding assays, the cultures were also grown in the fructose CSN induction medium supplemented with D-Ala at a final concentration of 20 mM for 10 days. There were three replicates for each strain. The mycelia of each sample were

harvested under vacuum, freeze-dried, and homogenized into fine powders. An equal amount of sample (20 mg each) was individually extracted with 500 μ l of methanol at 4°C for 2 days assisted with sonication treatments. The samples were then centrifuged at a maximum speed for 10 min, and the supernatants were collected for high-performance liquid chromatography (HPLC) analysis at 210 nm using a LC-20AD system (Shimadzu, Japan) equipped with an SPD-20A UV-visible (UV-Vis) detector and a C₁₈ reverse-phase column (particle size, 5 μ m; length, 4.6 by 250 mm; Agilent Eclipse XDB, USA). Aliquots (10- μ l aliquots) of samples were eluted with the deionized water (solution A) and acetonitrile (solution B, 65 to 100% acetonitrile) at a flow rate of 0.8 ml/min. Quantification of CsA production was performed by calibration to the standard curve generated using the CsA standard.

Bmt purification and substrate feeding. The intermediates and (4R)-4-[(E)-2-butenyl]-4-methyl-L-threonine (Bmt) produced by the polyketide synthase (PKS) pathway have no UV observance signals. To determine the compound structures, the Δ SimA mutant (having the highest accumulation level of Bmt) was grown in the fructose CSN induction medium in 1-liter flasks on a large scale (5 liters in total). The cultures were incubated at 25°C and 200 rpm for 2 weeks. The culture filtrates were collected, concentrated, and then extracted with methanol three times. Mycelial samples were freeze-dried and extracted with methanol also. The samples were first eluted with the preparative HPLC (LC-6AD; Shimadzu, Japan) system equipped with an Inertsil ODS C₁₈ column (particle size, 5 μ m; length, 10 by 250 mm; GL Sciences, Japan) and a FRC-10A fraction collector. The samples were eluted with deionized water (solution A) and acetonitrile (solution B, 5 to 100% acetonitrile) at a flow rate of 3 ml/min. The eluents were collected every 5 min, and the fractions were then subjected to purification using the Waters Acquity ultraperformance liquid chromatographic (UPLC) system equipped with an Acquity QDa MS (mass spectral) detector (Waters) and an Xbridge Prep C₁₈ column (particle size, 5 μ m; length, 19 by 150 mm; Waters, USA). The samples were eluted with 0.1% formic acid and acetonitrile (0 to 10 min, 2 to 8%; 10 to 15 min, 8 to 20%; 15 to 16 min, 20 to 95%) at a flow rate of 15 ml/min. The fractions containing the compound with the molecular weight of Bmt, and compounds b1 to b3 were collected. These samples were further purified with the system and eluted with 0.1% formic acid and acetonitrile (0 to 6.5 min, 10 to 12%; 6.5 to 12 min, 90%) at a flow rate of 10.8 ml/min. The purified samples were examined with an Agilent liquid chromatography (LC)-mass spectrometry (MS) system (6210 time of flight [TOF]/quadrupole time of flight [Q-TOF] LC-mass spectrometer; Agilent, USA) for purity analysis. After different trials, only Bmt was successfully collected. The compound (4 mg) was dissolved in D₂O for one-dimensional (1D) and 2D nuclear magnetic resonance (NMR) structure analysis with the Bruker Advanced III-500MHz system. After structure analysis, Bmt was used for feeding assays. Thus, the spores of Δ SimG, Δ SimI, and Δ SimJ mutants were inoculated in the fructose CSN induction medium (15 ml each in 100-ml flasks) supplemented with Bmt at a final concentration of 85 μ M. There were three replicates for each mutant, and the WT strain was inoculated in parallel for comparative analysis. After incubation for 2 weeks, the mycelia were harvested and extracted with methanol for HPLC analysis of CsA production.

Phylogenetic analysis. To determine the substrate specificity of the adenylation domains (A domains) and the potential cyclization role of the terminal condensation domain (C_T domain) of SimA, both the A and condensation (C) domains were retrieved based on the analysis with the program antiSMASH (ver. 3.0) (39) for phylogenetic analysis. Substrate-specific signatures of SimA A domains were predicted with the program NRPSpredictor2 (40). Additional C domains were also retrieved from the nonribosomal peptide synthetase (NRPS) DtxS1 for destruxin biosynthesis in *Metarhizium* spp. (27), and the beauvericin nonribosomal cyclodepsipeptide synthetase (BEAS) for the production of beauvericin in *B. bassiana* (29) as well as the cyclization C_T domains of *Penicillium aethiopicum* TqaA (21, 23) and *Emericella rugula* EcdA (41). The A- or C-domain sequences were aligned with the program Clustal X (ver. 2.1) (42), and neighbor-joining (NJ) trees were generated with the program MEGA 7.0 (43) using a Dayhoff model, pairwise deletion for gaps/missing data, and 1,000 bootstrap replications to test the phylogeny. Cyclophilin can bind CsA for cell protection/tolerance (3). Together with SimC, there are 10 cyclophilin genes encoded in the genome of *T. inflatum* (1). Different cyclophilins were selected from the close relatives of *T. inflatum* for phylogenetic analysis, including those from the insect pathogens *Beauveria bassiana* (44), *Metarhizium robertsii* (33), *Cordyceps militaris* (35), *Cordyceps cicadae* (34), and *Ophiocordyceps sinensis* (45). A NJ tree was generated using the same parameters indicated above.

Antifungal activity assay. CsA can bind cyclophilin to mediate antifungal activity (3). To test the effect of cyclophilin SimC and transporter SimD on cell protection, the WT, Δ SimA, Δ SimC, and Δ SimD strains of *T. inflatum* were grown on PDA amended with CsA or without CsA (supplemented at a saturated level in the medium). The colony sizes were then measured 12 days after inoculation, and the differences were compared for the WT and individual mutant strains to determine the effect of CsA on fungal growth. To determine the effect of CSN production on fungal competition with other fungi, both the WT and mutants of *T. inflatum* were inoculated on PDA plates (9 cm in diameter) in parallel for 3 days, and *A. flavus* spores (2 μ l of a suspension containing 1×10^7 spores/ml) were then inoculated in the middle of two colonies for pairing and competitive growth. Colony edge distances were measured to determine the differences between WT and *Aspergillus* and between mutants and *Aspergillus* after inoculation of *T. inflatum* for 1 or 3 weeks. Similar experiments were done by competition tests with other insect-pathogenic fungi, including *M. robertsii*, *C. militaris*, *C. cicadae*, and *B. brongniartii*. Each experiment has three replicates, and the difference between samples was examined using a Student's *t* test.

Insect bioassays. Insecticidal activity of CSNs was first demonstrated in mosquito larvae (32). To further determine the metabolite contribution to fungal virulence, insect bioassays were conducted by injection of the last instar larvae of wax moth. The spore suspensions of the WT, Δ SimA, Δ SimG, Δ SimL, and WT::SimL strains were prepared from the cultures grown on PDA plates for 4 weeks. The spore suspensions of the strains were placed in 0.05% Tween 20 to a final concentration of 2×10^6 spores/ml.

Insect larvae were injected individually in the second proleg with the spore suspension (10 μ l each). There were three replicates (15 insects per replicate) for each strain, and the experiments were repeated twice. The control insects were injected with 0.05% Tween 20. Mortality over time was recorded for each strain, and the median lethal time (LT₅₀) values were estimated and statistically compared for the WT and each mutant by Kaplan-Meier analysis with SPSS (ver. 22.0) (46).

SUPPLEMENTAL MATERIAL

Supplemental material for this article may be found at <https://doi.org/10.1128/mBio.01211-18>.

FIG S1, TIF file, 0.8 MB.

FIG S2, TIF file, 1.1 MB.

FIG S3, TIF file, 1.1 MB.

FIG S4, TIF file, 1.9 MB.

FIG S5, TIF file, 1.3 MB.

FIG S6, TIF file, 2.1 MB.

FIG S7, TIF file, 0.5 MB.

FIG S8, TIF file, 1.4 MB.

TABLE S1, PDF file, 0.1 MB.

TABLE S2, PDF file, 0.1 MB.

ACKNOWLEDGMENTS

We thank Junhai Huang and Yuanhong Shan for their help with LC-MS purification of Bmt and metabolite identification.

This work was supported by the National Natural Science Foundation of China (grant 31530001), Chinese Academy of Sciences (grants XDB11030100 and QYZDJ-SSW-SMC028), and National Key R&D Program of China (2017YFD0200400).

REFERENCES

- Bushley KE, Raja R, Jaiswal P, Cumbie JS, Nonogaki M, Boyd AE, Owensby CA, Knaus BJ, Elser J, Miller D, Di Y, McPhail KL, Spatafora JW. 2013. The genome of *Tolypocladium inflatum*: evolution, organization, and expression of the cyclosporin biosynthetic gene cluster. *PLoS Genet* 9:e1003496. <https://doi.org/10.1371/journal.pgen.1003496>.
- Borel JF, Feurer C, Gubler HU, Stähelin H. 1994. Biological effects of cyclosporin A: a new antilymphocytic agent. *Agents Actions* 43:179–186. <https://doi.org/10.1007/BF01986686>.
- Survase SA, Kagliwal LD, Annapure US, Singhal RS. 2011. Cyclosporin A—a review on fermentative production, downstream processing and pharmacological applications. *Biotechnol Adv* 29:418–435. <https://doi.org/10.1016/j.biotechadv.2011.03.004>.
- Lawen A, Zocher R. 1990. Cyclosporin synthetase. The most complex peptide synthesizing multienzyme polypeptide so far described. *J Biol Chem* 265:11355–11360.
- Weber G, Leitner E. 1994. Disruption of the cyclosporin synthetase gene of *Tolypocladium niveum*. *Curr Genet* 26:461–467. <https://doi.org/10.1007/BF00309935>.
- Hoffmann K, Schneider-Scherzer E, Kleinkauf H, Zocher R. 1994. Purification and characterization of eucaryotic alanine racemase acting as key enzyme in cyclosporin biosynthesis. *J Biol Chem* 269:12710–12714.
- di Salvo ML, Florio R, Paiardini A, Vivoli M, D'Aguanno S, Contestabile R. 2013. Alanine racemase from *Tolypocladium inflatum*: a key PLP-dependent enzyme in cyclosporin biosynthesis and a model of catalytic promiscuity. *Arch Biochem Biophys* 529:55–65. <https://doi.org/10.1016/j.abb.2012.11.011>.
- Offenzeller M, Su Z, Santer G, Moser H, Traber R, Memmert K, Schneider-Scherzer E. 1993. Biosynthesis of the unusual amino acid (4R)-4-[(E)-2-butenyl]-4-methyl-L-threonine of cyclosporin A. *J Biol Chem* 268:26127–26134.
- Offenzeller M, Santer G, Totschnig K, Su Z, Moser H, Traber R, Schneider-Scherzer E. 1996. Biosynthesis of the unusual amino acid (4R)-4-[(E)-2-butenyl]-4-methyl-L-threonine of cyclosporin A: enzymatic analysis of the reaction sequence including identification of the methylation precursor in a polyketide pathway. *Biochemistry* 35:8401–8412. <https://doi.org/10.1021/bi960224n>.
- Sangler JJ, Traber R, Buck RH, Hofmann H, Kobel H. 1990. Isolation of (4R)-4-[(E)-2-butenyl]-4-methyl-L-threonine, the characteristic structural element of cyclosporins, from a blocked mutant of *Tolypocladium inflatum*. *J Antibiot* 43:707–714. <https://doi.org/10.7164/antibiotics.43.707>.
- Fischer G, Wittmann-Liebold B, Lang K, Kiefhaber T, Schmid FX. 1989. Cyclophilin and peptidyl-prolyl cis-trans isomerase are probably identical proteins. *Nature* 337:476–478. <https://doi.org/10.1038/337476a0>.
- Wang P, Heitman J. 2005. The cyclophilins. *Genome Biol* 6:226. <https://doi.org/10.1186/gb-2005-6-7-226>.
- Zhou Y, Keyhani NO, Zhang Y, Luo Z, Fan Y, Li Y, Zhou Q, Chen J, Pei Y. 2016. Dissection of the contributions of cyclophilin genes to development and virulence in a fungal insect pathogen. *Environ Microbiol* 18:3812–3826. <https://doi.org/10.1111/1462-2920.13339>.
- Keller NP. 2015. Translating biosynthetic gene clusters into fungal armor and weaponry. *Nat Chem Biol* 11:671–677. <https://doi.org/10.1038/nchembio.1897>.
- Vilcinskis A, Kopacek P, Jegorov A, Vey A, Matha V. 1997. Detection of lipophorin as the major cyclosporin-binding protein in the hemolymph of the greater wax moth *Galleria mellonella*. *Comp Biochem Physiol* 117:41–45. [https://doi.org/10.1016/S0742-8413\(96\)00235-6](https://doi.org/10.1016/S0742-8413(96)00235-6).
- Fiolka MJ. 2008. Immunosuppressive effect of cyclosporin A on insect humoral immune response. *J Invertebr Pathol* 98:287–292. <https://doi.org/10.1016/j.jip.2008.03.015>.
- Margaritis A, Chahal PS. 1989. Development of a fructose based medium for biosynthesis of cyclosporin-A by *Beauveria nivea*. *Biotechnol Lett* 11:765–768. <https://doi.org/10.1007/BF01026093>.
- Keller NP, Turner G, Bennett JW. 2005. Fungal secondary metabolism—from biochemistry to genomics. *Nat Rev Microbiol* 3:937–947. <https://doi.org/10.1038/nrmicro1286>.
- Macheleidt J, Mattern DJ, Fischer J, Netzker T, Weber J, Schroeckh V, Valiante V, Brakhage AA. 2016. Regulation and role of fungal secondary metabolites. *Annu Rev Genet* 50:371–392. <https://doi.org/10.1146/annurev-genet-120215-035203>.
- Huang W, Shang Y, Chen P, Cen K, Wang C. 2015. Basic leucine zipper (bZIP) domain transcription factor MBZ1 regulates cell wall integrity, spore adherence, and virulence in *Metarhizium robertsii*. *J Biol Chem* 290:8218–8231. <https://doi.org/10.1074/jbc.M114.630939>.
- Gao X, Haynes SW, Ames BD, Wang P, Vien LP, Walsh CT, Tang Y. 2012.

- Cyclization of fungal nonribosomal peptides by a terminal condensation-like domain. *Nat Chem Biol* 8:823–830. <https://doi.org/10.1038/nchembio.1047>.
22. Butler AR, Bate N, Cundliffe E. 1999. Impact of thioesterase activity on tylosin biosynthesis in *Streptomyces fradiae*. *Chem Biol* 6:287–292. [https://doi.org/10.1016/S1074-5521\(99\)80074-X](https://doi.org/10.1016/S1074-5521(99)80074-X).
 23. Zhang J, Liu N, Cacho RA, Gong Z, Liu Z, Qin W, Tang C, Tang Y, Zhou J. 2016. Structural basis of nonribosomal peptide macrocyclization in fungi. *Nat Chem Biol* 12:1001–1003. <https://doi.org/10.1038/nchembio.2202>.
 24. Cheng YQ, Walton JD. 2000. A eukaryotic alanine racemase gene involved in cyclic peptide biosynthesis. *J Biol Chem* 275:4906–4911. <https://doi.org/10.1074/jbc.275.7.4906>.
 25. Zhang K, Li H, Cho KM, Liao JC. 2010. Expanding metabolism for total biosynthesis of the nonnatural amino acid L-homoalanine. *Proc Natl Acad Sci U S A* 107:6234–6239. <https://doi.org/10.1073/pnas.0912903107>.
 26. Spitteller P. 2015. Chemical ecology of fungi. *Nat Prod Rep* 32:971–993. <https://doi.org/10.1039/C4NP00166D>.
 27. Wang B, Kang Q, Lu Y, Bai L, Wang C. 2012. Unveiling the biosynthetic puzzle of destruxins in *Metarhizium* species. *Proc Natl Acad Sci U S A* 109:1287–1292. <https://doi.org/10.1073/pnas.1115983109>.
 28. Feng P, Shang Y, Cen K, Wang C. 2015. Fungal biosynthesis of the bibenzoquinone oosporein to evade insect immunity. *Proc Natl Acad Sci U S A* 112:11365–11370. <https://doi.org/10.1073/pnas.1503200112>.
 29. Xu Y, Orozco R, Wijeratne EM, Gunatilaka AA, Stock SP, Molnar I. 2008. Biosynthesis of the cyclooligomer depsipeptide beauvericin, a virulence factor of the entomopathogenic fungus *Beauveria bassiana*. *Chem Biol* 15:898–907. <https://doi.org/10.1016/j.chembiol.2008.07.011>.
 30. Wei G, Lai Y, Wang G, Chen H, Li F, Wang S. 2017. Insect pathogenic fungus interacts with the gut microbiota to accelerate mosquito mortality. *Proc Natl Acad Sci U S A* 114:5994–5999. <https://doi.org/10.1073/pnas.1703546114>.
 31. Fan Y, Liu X, Keyhani NO, Tang G, Pei Y, Zhang W, Tong S. 2017. Regulatory cascade and biological activity of *Beauveria bassiana* oosporein that limits bacterial growth after host death. *Proc Natl Acad Sci U S A* 114:E1578–E1586. <https://doi.org/10.1073/pnas.1616543114>.
 32. Weiser J, Matha V. 1988. The insecticidal activity of cyclosporines on mosquito larvae. *J Invertebr Pathol* 51:92–93. [https://doi.org/10.1016/0022-2011\(88\)90092-4](https://doi.org/10.1016/0022-2011(88)90092-4).
 33. Hu X, Xiao G, Zheng P, Shang Y, Su Y, Zhang X, Liu X, Zhan S, St Leger RJ, Wang C. 2014. Trajectory and genomic determinants of fungal-pathogen speciation and host adaptation. *Proc Natl Acad Sci U S A* 111:16796–16801. <https://doi.org/10.1073/pnas.1412662111>.
 34. Lu Y, Luo F, Cen K, Xiao G, Yin Y, Li C, Li Z, Zhan S, Zhang H, Wang C. 2017. Omics data reveal the unusual asexual-fruitlet nature and secondary metabolic potentials of the medicinal fungus *Cordyceps cicadae*. *BMC Genomics* 18:668. <https://doi.org/10.1186/s12864-017-4060-4>.
 35. Zheng P, Xia Y, Xiao G, Xiong C, Hu X, Zhang S, Zheng H, Huang Y, Zhou Y, Wang S, Zhao GP, Liu X, St Leger RJ, Wang C. 2011. Genome sequence of the insect pathogenic fungus *Cordyceps militaris*, a valued traditional Chinese medicine. *Genome Biol* 12:R116. <https://doi.org/10.1186/gb-2011-12-11-r116>.
 36. Shang Y, Xiao G, Zheng P, Cen K, Zhan S, Wang C. 2016. Divergent and convergent evolution of fungal pathogenicity. *Genome Biol Evol* 8:1374–1387. <https://doi.org/10.1093/gbe/eww082>.
 37. Xia YL, Luo FF, Shang YF, Chen PL, Lu YZ, Wang CS. 2017. Fungal cordycepin biosynthesis is coupled with the production of the safeguard molecule pentostatin. *Cell Chem Biol* 24:1479–1489. <https://doi.org/10.1016/j.chembiol.2017.09.001>.
 38. Crooks GE, Hon G, Chandonia JM, Brenner SE. 2004. WebLogo: a sequence logo generator. *Genome Res* 14:1188–1190. <https://doi.org/10.1101/gr.849004>.
 39. Weber T, Blin K, Duddela S, Krug D, Kim HU, Brucoleri R, Lee SY, Fischbach MA, Muller R, Wohlleben W, Breitling R, Takano E, Medema MH. 2015. antiSMASH 3.0—a comprehensive resource for the genome mining of biosynthetic gene clusters. *Nucleic Acids Res* 43:W237–W243. <https://doi.org/10.1093/nar/gkv437>.
 40. Röttig M, Medema MH, Blin K, Weber T, Rausch C, Kohlbacher O. 2011. NRPSpredictor2—a web server for predicting NRPS adenylation domain specificity. *Nucleic Acids Res* 39:W362–W367. <https://doi.org/10.1093/nar/gkr323>.
 41. Cacho RA, Jiang W, Chooi YH, Walsh CT, Tang Y. 2012. Identification and characterization of the echinocandin B biosynthetic gene cluster from *Emericella rugulosa* NRRL 11440. *J Am Chem Soc* 134:16781–16790. <https://doi.org/10.1021/ja307220z>.
 42. Larkin MA, Blackshields G, Brown NP, Chenna R, McGettigan PA, McWilliam H, Valentin F, Wallace IM, Wilm A, Lopez R, Thompson JD, Gibson TJ, Higgins DG. 2007. Clustal W and Clustal X version 2.0. *Bioinformatics* 23:2947–2948. <https://doi.org/10.1093/bioinformatics/btm404>.
 43. Kumar S, Stecher G, Tamura K. 2016. MEGA7: Molecular Evolutionary Genetics Analysis version 7.0 for bigger datasets. *Mol Biol Evol* 33:1870–1874. <https://doi.org/10.1093/molbev/msw054>.
 44. Xiao G, Ying SH, Zheng P, Wang ZL, Zhang S, Xie XQ, Shang Y, St Leger RJ, Zhao GP, Wang C, Feng MG. 2012. Genomic perspectives on the evolution of fungal entomopathogenicity in *Beauveria bassiana*. *Sci Rep* 2:483. <https://doi.org/10.1038/srep00483>.
 45. Hu X, Zhang YJ, Xiao GH, Zheng P, Xia YL, Zhang XY, St Leger RJ, Liu XZ, Wang CS. 2013. Genome survey uncovers the secrets of sex and lifestyle in caterpillar fungus. *Chin Sci Bull* 58:2846–2854. <https://doi.org/10.1007/s11434-013-5929-5>.
 46. Chen YX, Feng P, Shang YF, Xu YJ, Wang CS. 2015. Biosynthesis of non-melanin pigment by a divergent polyketide synthase in *Metarhizium robertsii*. *Fungal Genet Biol* 81:142–149. <https://doi.org/10.1016/j.fgb.2014.10.018>.